Applied Radiation and Isotopes 201 (2023) 110991

Contents lists available at ScienceDirect

Applied Radiation and Isotopes

journal homepage: www.elsevier.com/locate/apradiso

In-toto non-destructive assay methodology for the elimination of metallic waste from particle accelerators after melting

Patrycja Dyrcz *, Nabil Menaa, Matteo Magistris, Chris Theis, Luca Bruno, Gerald Dumont, Renaud Charousset

CERN, CH-1211 Meyrin, Switzerland

ARTICLE INFO

Keywords:
Radioactive waste characterization
Gamma spectrometry
Geometry optimization
Geometry modelling
Melting
Radiochemical analysis

ABSTRACT

Melting of metallic waste reduces the waste volume, allows more accurate radiological characterization, and minimizes handling at the waste production site. This paper proposes a new non-destructive assay methodology to radiologically characterize low- and intermediate-level (LILW) waste before melting. A non-destructive assay technique is developed and qualified using geometry optimization technique and sample analysis after melting. Additionally, we present an operational methodology to predict the activity values of the major gamma emitters based on the average dose rate measurements.

1. Introduction

The European Organization for Nuclear Research's (CERN) accelerator complex uses a variety of particle types and energies. It is characterized by a wide range of different radiation fields, that can induce radioactivity in the machine components and surrounding material. If the activated material cannot be reused or recycled, it needs to be disposed of in dedicated final repositories. The radioactive waste produced at CERN is disposed of in France or Switzerland in accordance with the existing elimination pathways following the tripartite agreement between CERN, France and Switzerland (Host States) (Accord, 2011).

Melting of metallic radioactive waste offers a number of advantages: volume reduction, immobilization of contamination (if present) and radioactivity homogenization. In the present paper, we introduce a new characterization methodology that allows the safe disposal of legacy low- and intermediate-level (LILW) waste produced at CERN before melting. The radiological characterization process relies on extensive Monte Carlo and analytical calculations in order to perform the radiological inventory predictions for solid metallic waste items.

The radiological characterization presents several challenges. Items of waste, that are candidates for elimination as LILW, present contact dose-rate levels up to 2 mSv/h, a radiation level which is challenging in terms of operational radiation protection during the phases of handling and measurements. In addition, these waste items often exhibit highly heterogeneous activity distributions. Hence, it is necessary to estimate the accuracy of the activity values that are obtained by *in-toto* gamma spectrometry (GS) when assuming a uniform activity distribution. To this end, we propose a novel Non-Destructive Assay (NDA) technique that estimates and reduces the uncertainties introduced by the uniform activity model. We use geometry model optimization to quantify the expected activity concentration values to the best of our knowledge using multi-line and multi-count consistency constraints as described in the rest of this paper.

Section 2.1 gives a general overview of the primary radioactive waste candidates for disposal after melting. In Sections 2.2 and 2.3, we describe the new operational methodology to predict the activity concentration of the main gamma emitter (^{60}Co), as well as the new NDA technique using the optimization approach. Additionally, the experimental comparison of the activity values before and after melting is presented.

2. Materials and methods

2.1. LILW radioactive waste at CERN

A significant amount of the radioactive waste collected from the different CERN operations (e.g. dismantling and maintenance) are metallic components, consisting primarily of steel, copper and aluminium. The waste that will be shipped to the melting facility has to consist of stainless steel, black steel or cast iron and galvanized steel. Waste will be packed in containers of 2.7 m^3 or 4 m^3, or unitary pieces that would fit in a 20-feet shipping container. The waste selection process starts with the so-called pre-selection phase. In this step, one segregates the

* Corresponding author.
E-mail address: patrycja.kinga.dyrcz@cern.ch (P. Dyrcz).

https://doi.org/10.1016/j.apradiso.2023.110991
Received 1 May 2023; Received in revised form 16 August 2023; Accepted 17 August 2023
Available online 19 August 2023

waste based on the dose rate levels and verifies which waste could be subjected to further processing. Hence, the waste with the maximum dose at contact between 10 μSv/h and 2 mSv/h is classified as LILW waste candidate. Subsequently, this waste is measured using a non-destructive X-ray fluorescence (XRF) technique in order to determine the elemental composition. Consequently, the waste consisting of stainless steel, cast iron etc. can be grouped and pre-packaged in containers of 2.7 m^3 or 4 m^3. The LILW waste which is covered by the present study complies with the acceptance criteria of the melting facility, such as: (1) the dose rate of the primary waste is lower than 2 mSv/h at contact, (2) the loose surface contamination is <4 Bq/cm^2 for gamma and beta emitters and <0.4 Bq/cm^2 for alpha emitters, and (3) the maximum activity of gamma and beta emitters is 20 kBq/g.

2.2. Primary waste selection phase

The activity concentration of the main gamma emitter (^{60}Co), and consequently the total beta-gamma specific activity was predicted by applying the Scaling Factor (SF) approach (Dyrcz, 2022). This methodology is valid for solid metallic LILW waste generated at CERN under the assumption that ^{60}Co is the dominant gamma emitter that contributes to the dose rate in the waste item, where the decay time is more than 3 years. This preliminary prediction of the total beta-gamma activity values was implemented in the pre-packaging phase of the radioactive waste in an operationally efficient manner, taking into account the radiation protection dose optimization objectives following the ALARA (As Low As Reasonably Achievable) (Forkel-Wirth et al., 2013) principle and the acceptance criteria of the melting facility. The methodology was designed to be reasonably conservative. It is based on the average dose rate (AVG-DR) measurements of the ferrous LILW waste generated at CERN. In order to convert the AVG-DR values of the waste items into ^{60}Co activities, two approaches were investigated. The first approach is based on the experimental correlation between the ratio of the specific activity of ^{60}Co and the AVG-DR as a function of the apparent density of the waste item. The other approach focuses on accurate geometry modelling of the waste item using a radiation protection code MERCURAD from Mirion Technologies (Canberra).

The AVG-DR methodology allows the estimation of the total beta-gamma specific activity concentrations of pre-selected waste based on the measured average dose rate and apparent density. In order to establish the correlation between the specific activity and average dose rate at 40 cm, we measured 35 individual representative waste items prior to their conditioning into output waste packages, for a large range of the apparent density values and dose rate levels. All items were also measured using GS. The acquisitions were carried out using High Purity Germanium detectors (Falcon 5000) from Mirion Technologies (Canberra) in a dedicated area where the background dose rate varies between 0.07 and 0.1 μSv/h. During the acquisition step, the waste-to-detector distance was selected to have a maximum allowed dead time less than 15% for all measured waste items and the acquisition live time varied from 10'000 to 72'000 s. The dose rate measurements were carried out using Dose Rate Meter 6150AD 6/H,[1] with a dynamic range from 0.1 μSv/h to 10 mSv/h and an energy range from 60 keV to 1.3 MeV. For waste items, which present a magnetic field, we used the RadEye,[2] device from ThermoFisher Scientific that was tested in the presence of magnetic field strengths up to 300 mT. The dose rates were measured at multiple points around the waste at 40 cm and scanning (only for 6150AD 6/H device), while the apparent density was estimated by taking the ratio of the mass and apparent envelope volume of the waste.

MERCURAD,[3] was used for the calculation of the gamma dose equivalent rate. It is based on the Mercure-6 (Assad et al., 2000) Kernel, developed by CEA (French Atomic Energy and Alternative Energies Commission). MERCURAD allows the modelling of complex geometries including hollow objects such as pipes and ion pumps. To compute the dose equivalent rate, the MERCURAD sensors were set at 40 cm from the modelled waste items. MERCURAD allows calculating the dose rate response for a source term corresponding to 1 Bq/g allowing us to convert a measured dose rate into an equivalent specific activity of ^{60}Co in our case.

2.3. Radiological analysis of waste packages and unitary items

The developed methodology was validated using *in-toto* GS measurements of both the individual waste items, as well as the waste packages containing the items. The quantification of the Easy-To-Measure (ETM) radionuclides (TECDOC IAEA, 2007) was performed by GS, under the assumption of homogeneous activity distribution within the item. However, due to the activation mechanisms, some waste can have heterogeneous activation patterns.

GS measurements on LILW items present several challenges during both the acquisition and the analysis steps. The former challenges relate to the high counting rate effects, the long counting time required to meet the Minimum Detectable Activity (MDA) requirements, available physical space, and the necessity to count from multiple faces. The latter challenges are due to the difficulty to model the geometry and combine the multiple count results. A significant parameter of the acquisition step is the system dead time. In order to avoid the spectrum distortions, we limited the dead time value to ~15% nominally. However, in the case of the detector-waste distance of 1.9 m, the dead time reached 19% due to insufficient physical space around the waste item. The average dose rate at contact was 98 μSv/h, and the maximum dose rate was 260 μSv/h.

Additionally, the acquisition time and geometry need to be set in such a way to ensure that the MDA values are below the LILW waste declaration thresholds (ANDRA, 2013b,a) for the expected ETM radionuclides. The main acquisition parameters for the waste packages and unitary items can be found in Tables 1 and 2 respectively. For each GS acquisition of each face (or count), we produced a reference efficiency calibration curve by applying the "Complex Box" In Situ Object Counting System (ISOCS) (Bronson, 1997) geometry template and assuming a uniform source distribution in the material matrix. The activity values were determined using Genie 2000.[4]

When GS measurements are performed on waste items, the knowledge of the geometry model parameters, including dimensions, position with respect to the detector, material composition, and activity distribution (hotspots) is often limited, especially for the two last parameters (Kaminski et al., 2014; Bronson, 2008). However, during the GS analysis, it is more practical to quantify the ETM radionuclides under the assumption of homogeneous activity distributions within a measured waste. This assumption might lead to inaccuracies in the estimation of the ETM activity values. In order to determine the uncertainties of the measured activities, due to the variation of the waste geometry parameters, such as dimensions and heterogeneous source distribution we used ISOCS Uncertainty Estimator (IUE) (Menaa et al., 2011) and an in-house developed tool named Geometry Uncertainty Reduction Utility (GURU) (Frosio et al., 2020; Dyrcz et al., 2021). The latter consists of two modules. One quantifies the geometry model

[1] https://www.automess.de/assets/documents/en/Prospekt_6150AD_E.pdf last visited on 15 August 2023.

[2] https://www.thermofisher.com/order/catalog/product/4250671 last visited on 15 August 2023.

[3] https://www.mirion.com/products/mercurad-3d-simulation-software-for-dose-rate-calculation last visited on 15 August 2023.

[4] https://www.mirion.com/products/technologies/spectroscopy-scientific-analysis/gamma-spectroscopy/gamma-spectroscopy-software/lab-applications/genie-spectroscopy-software-suite last visited on 15 August 2023.

Table 1
Main acquisition setup parameters of the GS measurements for waste packages. The acquisition live time for all waste packages was 10'000 s.

Waste package #	WP1 CR-125219	WP2 CR-064156	WP3 CR-139253	WP4 CR-139254	WP5 CR-139255
Dead time (%)	13.5–18.6	11–13.4	8.2–11.2	3.8–4.8	4.4–6
Distance (m)	1.92	2.8–2.95	3.4–3.65	3.6–3.76	3.8–4.25
Maximum dose rate at contact (μSv/h)	260	316	250	147	280
AVG-DR at 40 cm (μSv/h)	41.1	56	62	26.7	40

Table 2
Main acquisition setup parameters of the GS measurements for unitary items.

Unitary item #	UP1 CR-063808	UP2 CR-W13057	UP3 CR-065037	UP4 CR-065038
Dead time (%)	1.9–7.7	0.8–3.8	0.7–66	1.7–1.9
Distance (m)	1.24–1.84	1	2.2	2.2
Maximum dose rate at contact (μSv/h)	200	43	15	57
AVG-DR at 40 cm (μSv/h)	9	2	2	4
Acquisition live time (s)	900		1800	

uncertainties and the other reduces them by combining the GS results in order to identify the best estimate model that best describes the "actual" geometry of the waste. By varying the geometry parameters, a set of perturbed efficiency calibration curves were produced. These curves were used to evaluate activity results as a function of the geometry parameters. In order to perform an optimization (i.e. determine the best geometry models), the following constraints should be fulfilled (Bronson, 1997): multi-count consistency is the requirement that multiple GS measurements carried out at different locations should give the same value of the measured activity of the item. Additionally, the calculated activity values for each emission line of a radionuclide should be consistent. Knowing the activity values from each detector count for a reference model, we can correct these activities by the ratio of efficiencies as

$$\forall i, j, k, A_i^k(j) = \frac{\epsilon_{ref}^k(E)}{\epsilon_i^k(E)} A_{ref}^k(j). \quad (1)$$

$A_i^k(j)$ is the calculated activity for the radionuclide with emission j using model i for the face k. $A_{ref}^k(j)$ represents the calculated activity with the reference model. The efficiencies $\epsilon_{ref}^k(E)$ and $\epsilon_i^k(E)$ correspond to the reference model and model i at energy E of emission j from the face (detector) k.

Using Eq. (1) a set of activities can be calculated for each radionuclide emission, in each model and detector. Then using the line and count consistencies, we match the activities between the different detectors. To this end, we construct a Figure Of Merit (FOM) as follows for each gamma emission j and model i:

$$FOM_i(j) = \sum_{k=1}^{K} (A_i^k(j) - < A_i(j) >)^2, \quad (2)$$

where $A_i^k(j)$ is the activity of the radionuclide with associated gamma emission j using model i for face k. $< A_i(j) >$ is the average over K faces for emission j using model i, which is defined as $< A_i(j) >= \sum_{k=1}^{K} \frac{A_i^k(j)}{K}$.

The user needs to select the gamma lines of interest, among the ones identified in all faces of the GS measurement results. Then, one can calculate a Rank (as given in Eq. (3)) for each gamma emission line and model by summing the sub-ranks ($subRank_i^j$) according to the FOM value. Namely, the sub-rank $subRank_i^j$ is obtained by ranking the $FOM_i(j)$. Hence for all models n, the best model for each gamma emission line is assigned to a sub-rank # 1, the second best to # 2, etc.

$$Rank_i = \sum_{j=0}^{J} subRank_i^j, \quad (3)$$

where J is the number of common gamma emission lines formed for each face. The model with the minimum $Rank_i$ is considered as the best model.

2.4. Melting of primary waste

The primary waste batch of 19 m^3 was shipped to the melting facility and transformed into three melting baths of around 4 tons each. Two samples were taken from each bath, which resulted in a total of six samples after melting. The samples are representative to the corresponding bath due to the melting homogenization process via continuous heat convection currents inside the melting bath. In other words, the activity is uniformly distributed within the bath, which shows the power and accuracy of sampling and subsequent analyses. In order to avoid cross-contamination with waste originating from other producers, the melting process was dedicated to CERN waste using a new and dedicated refractory lining.

3. Results and discussion

3.1. Waste selection using the measured AVG-DR and ^{60}Co activity correlation method

We produced a curve of the ratio between the ^{60}Co specific activity and the AVG-DR at 40 cm as a function of the apparent density as shown in Fig. 1. A fit was performed to produce a penalizing fit function at the 50% confidence level. The data points represent the measurements (GS and dose rate mapping) for hollow (e.g. pipes), ion pumps, containers and other waste items considered as LILW waste candidates. The fit (red line) equation is given by the equation (5.07/Apparent density + 12.31) and a 0.92 value of R^2 coefficient. Whereas, the penalizing fit (blue line) takes the form of (5.26/Apparent density + 17.31) and R^2 of 1.

3.2. Waste selection using the computed AVG-DR and ^{60}Co activity correlation method

Similarly, to the previous Subsection, we present the results of the method using the transport code MERCURAD (see Fig. 2). The results show that the ratio of the estimated ^{60}Co activities, using MERCURAD to the GS results, is consistent with unity in most of the cases. In some cases, we noticed that the MERCURAD results are within 50% of the expected activity value given by GS.

Although, this method yields to an accuracy of 50%, it is not selected as the method to be used to estimate the ^{60}Co specific activities during the waste selection phase as it requires a specific level of operator training in setting up the geometry and interpreting the output files of the MERCURAD software, and it is more prone to human errors.

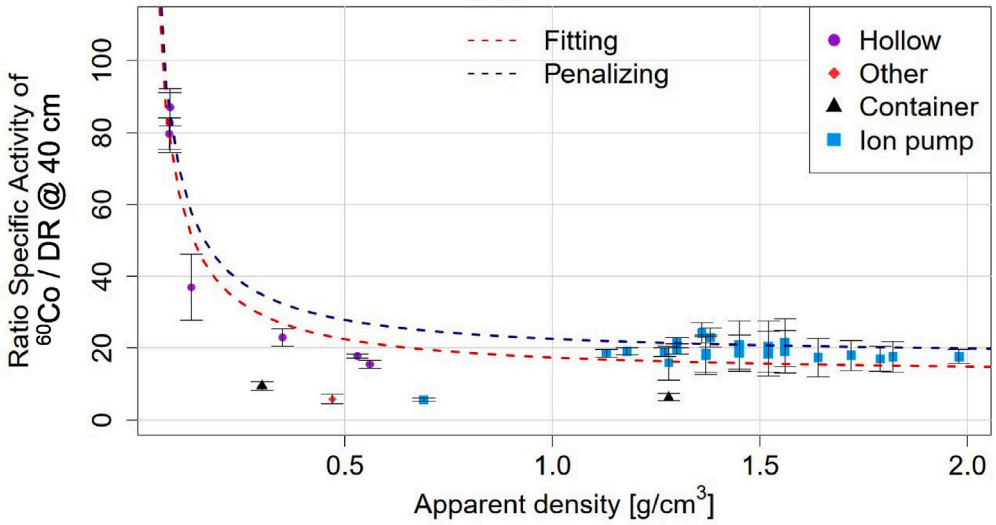

Fig. 1. The ratio of the specific activity of ^{60}Co and AVG-DR at 40 cm as a function of the apparent density.

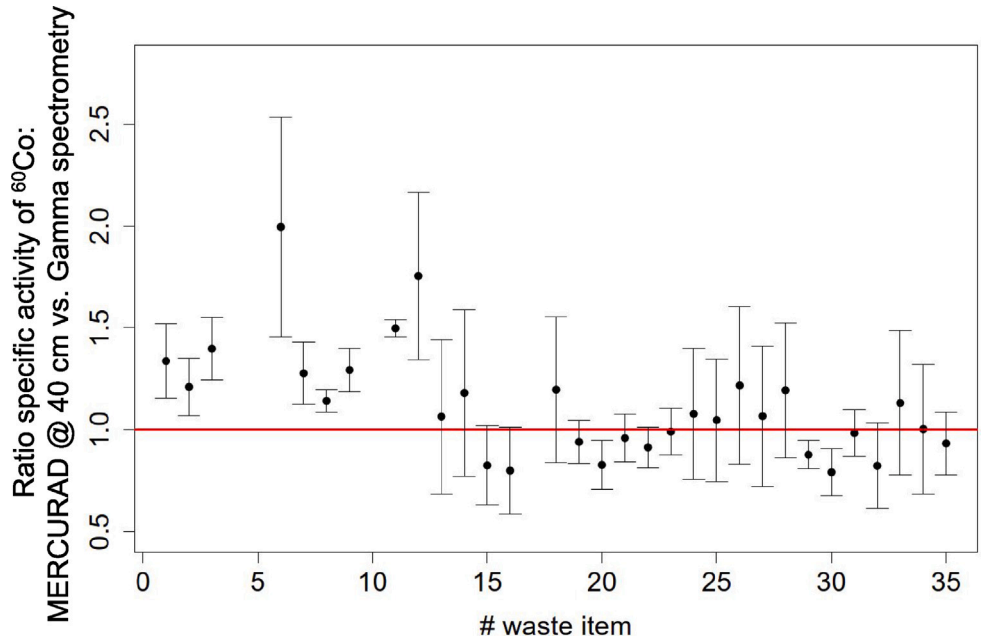

Fig. 2. Ratio of the estimated ^{60}Co activities using MERCURAD and AVG-DR measurements at 40 cm to the GS results. The uncertainties are given at 1 σ.

3.3. Comparison of AVG-GS and geometry optimization results for primary waste

Table 3 presents the multi-count GS activity differences of the reference geometry models respectively for one of the waste packages with a net mass of 1390 kg and an apparent density of 0.596 g/cm^3. The GS analysis results do not include the systematic uncertainties due to geometry modelling of the measured waste package. It needs to be noted that the activities of ^{44}Ti and ^{44}Sc radionuclides are estimated independently, not taking into account that they are in secular equilibrium ^{44}Sc < ^{44}Ti. The ratio of the ^{60}Co activity concentrations estimated via the AVG-DR methodology and AVG-GS measurements of the output waste packages ranges from 1.4 to 3.

The GURU framework enables varying the relative source concentrations of the hot spots (referred to as the contrast). The contrast value is estimated as the ratio of the highest and lowest activities between two opposite faces assuming uniform activity source distribution. The optimization process was performed over two faces at a time. The contrast parameters were varied from 1 to 10, from 1 to 100 or from 1 to 150, which depended on the heterogeneity of the assay waste package. An example of the activity ratios of the two opposite faces from the GS measurements with a uniform activity source distribution (reference model) is shown in Fig. 3.

It is noted that after geometry optimization (see Fig. 3), the activity ratios become very close to unity, hence showing the usefulness and effectiveness of the methodology for benchmarking purposes. The activity uncertainty of the average value is calculated as the square root of the quadratic sum of uncertainties corresponding to a single face. In the following Tables 4–8, the average activity values of the reference and optimized models over two and four opposite faces for each waste package are presented. The reported uncertainty of the reference activity results does not include the geometry model uncertainty due to the not well-known parameters while NA indicates that geometry optimization was not performed.

Table 3
List of identified radionuclides with the activity values for the four faces of the waste package WP1 CR-125219. The uncertainties are quoted at 1 σ (relative uncertainties). MDA values are in *italic*.

	^{60}Co (Bq/g)	^{22}Na (Bq/g)	^{42}K (Bq/g)	^{44}Sc (Bq/g)	^{44}Ti (Bq/g)	^{54}Mn (Bq/g)
FACE 1	2.65E+02 (3%)	5.68E−01 (11%)	1.64E−01 (20%)	1.08E+00 (6%)	*4.700E+00*	7.68E−01 (19%)
FACE 2	2.23E+02 (3%)	1.44E+00 (6%)	5.07E−01 (9%)	2.43E+00 (6%)	3.04E+00 (25%)	2.38E+00 (9%)
FACE 3	3.29E+02 (3%)	3.39E−01 (8%)	1.72E−01 (22%)	1.07E+00 (6%)	*4.982E+00*	1.39E+00 (6%)
FACE 4	2.71E+02 (3%)	9.81E−01 (5%)	2.59E−01 (14%)	1.47E+00 (6%)	*4.933E+00*	1.78E+00 (8%)
Activity ratio between faces 1 and 3	1.24 (± 0.06)	1.68 (± 0.22)	1.05 (± 0.31)	1.01 (± 0.09)		1.81 (± 0.37)
Activity ratio between faces 2 and 4	1.22 (± 0.06)	1.46 (± 0.12)	1.96 (± 0.33)	1.66 (± 0.14)		1.34 (± 0.16)
Average activity over all faces	2.72E+02 (2%)	8.31E−01 (4%)	2.76E−01 (7%)	1.51E+00 (3%)		1.58E+00 (5%)
Estimated activity via AVG-DR	3.74E+02					

Table 4
Average activity values over two, four faces for reference and optimized models with uncertainties given at 1 σ for WP1.

	WP1 CR-125219								
Radionuclide (Bq/g)	REFERENCE			OPTIMIZED			OPTIMIZED/REFERENCE		
	Faces 1–3	Faces 2–4	Four faces	Faces 1–3	Faces 2–4	Four faces	Faces 1–3	Faces 2–4	Four faces
^{60}Co	2.97E+02 (2%)	2.47E+02 (2%)	2.72E+02 (2%)	3.23E+02 (2%)	3.29E+02 (2%)	3.26E+02 (2%)	1.09 (±0.04)	1.33 (±0.05)	1.20 (±0.03)
^{22}Na	4.54E−01 (7%)	1.21E+00 (4%)	8.31E−01 (4%)	5.23E−01 (7%)	1.63E+00 (4%)	1.07E+00 (3%)	1.15 (±0.11)	1.35 (±0.08)	1.29 (±0.06)
^{42}K	1.68E−01 (15%)	3.83E−01 (8%)	2.76E−01 (7%)	2.14E−01 (15%)	5.57E−01 (9%)	3.86E−01 (7%)	1.28 (±0.27)	1.45 (±0.17)	1.40 (±0.14)
^{44}Sc	1.08E+00 (4%)	1.95E+00 (4%)	1.51E+00 (3%)	1.07E+00 (4%)	2.37E+00 (4%)	1.72E+00 (3%)	0.99 (±0.06)	1.21 (±0.07)	1.14 (±0.05)
^{44}Ti					NA				
^{54}Mn	1.08E+00 (8%)	2.08E+00 (6%)	1.58E+00 (5%)	1.22E+00 (10%)	3.09E+00 (6%)	2.15E+00 (5%)	1.13 (±0.15)	1.49 (±0.12)	1.36 (±0.09)

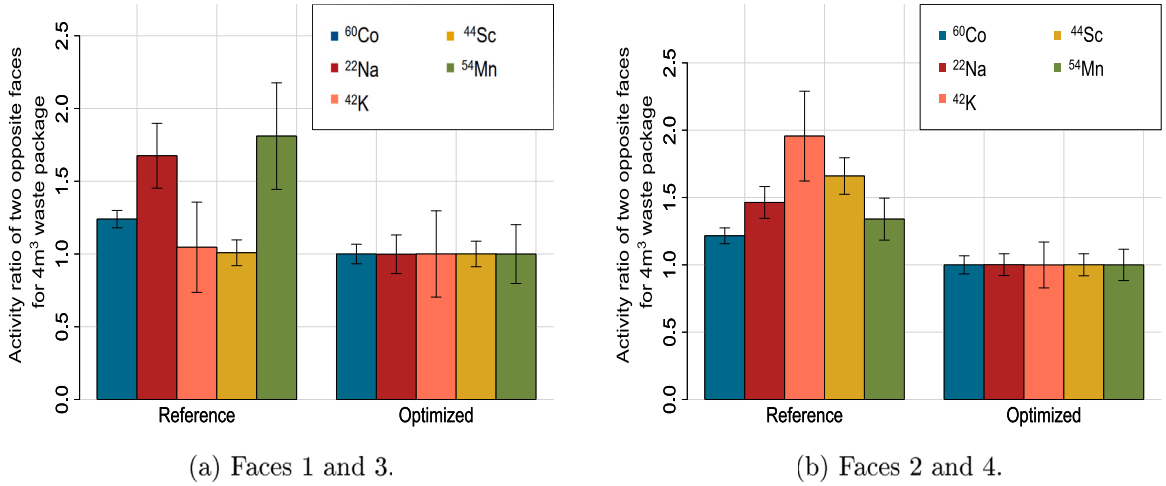

(a) Faces 1 and 3. (b) Faces 2 and 4.

Fig. 3. Activity ratios for opposite faces before and after optimization. The contrast ranges from 1 to 10 for WP1 CR-125219.

The list of identified radionuclides with the associated activity values of the reference models for one representative unitary item is presented in Table 9.

Similarly, the optimization process was performed on each unitary item over two faces at a time. The contrast parameters were varied from 1 to 10 and 1 to 50 depending on the heterogeneity of the unitary item waste. Fig. 4 presents an example of the activity ratios of the two opposite faces for the reference and optimized models where the contrast was varied from 1 to 10 for faces 1 and 3, and 1 to 50 for faces 2 and 4. The activity values using geometry optimization technique of the two opposite faces are consistent as the corresponding activity ratios are close to unity.

The following Tables 10–12 present the average activity values of the reference and optimized models over two, and four opposite faces, when applicable, for all the unitary items.

We notice that the relative differences between the optimized and average four faces measurements, assuming uniform activity distribution, for ^{60}Co range from about 20% to 30% for materials packaged in containers, and only about 10% to 15% for unitary items. For other radionuclides, the optimized method generally yields larger values compared to the average four faces measurement. The obtained results allow confirming that the activity average over the faces, assuming uniform activity distribution, is suitable compared with the geometry optimization results.

3.4. Comparison of AVG-GS results after melting

The activity values of the six samples extracted after melting are given in Table 13 while Table 14 presents the AVG-GS activity values for identified radionuclides before and after melting. For the activity values before melting, the GS results are averaged over the faces and

Table 5
Average activity values over two, four faces for reference and optimized models with uncertainties given at 1 σ for WP2.

WP2 CR-064156									
Radionuclide (Bq/g)	REFERENCE			OPTIMIZED			OPTIMIZED/REFERENCE		
	Faces 1–3	Faces 2–4	Four faces	Faces 1–3	Faces 2–4	Four faces	Faces 1–3	Faces 2–4	Four faces
^{60}Co	3.10E+02 (1%)	3.55E+02 (1%)	3.33E+02 (1%)	3.67E+02 (1%)	4.26E+02 (1%)	3.97E+02 (1%)	1.18 (±0.02)	1.20 (±0.02)	1.19 (±0.02)
^{22}Na	2.43E+00 (2%)	3.18E+00 (2%)	2.81E+00 (2%)	2.68E+00 (2%)	2.90E+00 (2%)	2.79E+00 (2%)	1.10 (±0.04)	0.91 (±0.03)	0.99 (±0.02)
^{42}K	7.86E−01 (13%)	5.77E−01 (6%)	6.82E−01 (8%)	8.15E−01 (11%)	6.55E−01 (6%)	7.35E−01 (7%)	1.04 (±0.18)	1.14 (±0.10)	1.08 (±0.11)
^{44}Sc	4.41E+00 (2%)	3.55E+00 (3%)	3.98E+00 (2%)	5.28E+00 (2%)	4.67E+00 (3%)	4.97E+00 (2%)	1.20 (±0.04)	1.31 (±0.06)	1.25 (±0.03)
^{44}Ti	1.21E+01 (8%)	NA		2.40E+01 (10%)	NA		1.99 (±0.26)	NA	
^{54}Mn	1.25E+01 (2%)	2.63E+01 (2%)	1.94E+01 (2%)	1.52E+01 (2%)	2.93E+01 (2%)	2.22E+01 (2%)	1.22 (±0.04)	1.12 (±0.03)	1.15 (±0.03)
^{57}Co	1.41E+00 (15%)	1.80E+00 (7%)	1.60E+00 (5%)	2.78E+00 (8%)	2.34E+00 (7%)	2.56E+00 (5%)	1.97 (±0.21)	1.30 (±0.13)	1.60 (±0.12)

Table 6
Average activity values over two, four faces for reference and optimized models with uncertainties given at 1 σ for WP3.

WP3 CR-139253									
Radionuclide (Bq/g)	REFERENCE			OPTIMIZED			OPTIMIZED/REFERENCE		
	Faces 1–3	Faces 2–4	Four faces	Faces 1–3	Faces 2–4	Four faces	Faces 1–3	Faces 2–4	Four faces
^{60}Co	2.86E+02 (1%)	3.34E+02 (1%)	3.10E+02 (1%)	4.23E+02 (1%)	4.05E+02 (1%)	4.14E+02 (1%)	1.48 (±0.03)	1.21 (±0.02)	1.34 (±0.02)
^{22}Na	NA								
^{42}K	4.93E−01 (7%)	6.18E−01 (7%)	5.55E−01 (5%)	6.57E−01 (7%)	7.11E−01 (7%)	6.84E−01 (5%)	1.33 (±0.13)	1.15 (±0.11)	1.23 (±0.09)
^{44}Sc	3.06E+00 (2%)	3.44E+00 (2%)	3.25E+00 (2%)	2.82E+00 (2%)	4.24E+00 (2%)	4.03E+00 (2%)	1.25 (±0.04)	1.23 (±0.04)	1.24 (±0.03)
^{54}Mn	1.08E+00 (5%)	1.45E+00 (4%)	1.26E+01 (3%)	6.84E−01 (9%)	1.49E+00 (14%)	1.09E+00 (10%)	0.63 (±0.06)	1.03 (±0.15)	0.86 (±0.09)

Table 7
Average activity values over two, four faces for reference and optimized models with uncertainties given at 1 σ for WP4.

WP4 CR-139254									
Radionuclide (Bq/g)	REFERENCE			OPTIMIZED			OPTIMIZED/REFERENCE		
	Faces 1–3	Faces 2–4	Four faces	Faces 1–3	Faces 2–4	Four faces	Faces 1–3	Faces 2–4	Four faces
^{60}Co	1.70E+02 (1%)	1.55E+02 (1%)	1.62E+02 (1%)	2.08E+02 (1%)	1.85E+02 (1%)	1.97E+02 (1%)	1.23 (±0.02)	1.20 (±0.02)	1.21 (±0.02)
^{22}Na	NA								
^{42}K	NA								
^{44}Sc	1.16E+00 (3%)	1.23E+00 (3%)	1.19E+00 (2%)	1.18E+00 (4%)	1.22E+00 (4%)	1.20E+00 (2%)	1.02 (±0.05)	0.99 (±0.05)	1.01 (±0.03)
^{54}Mn	NA								

over the 5 waste packages and 4 unitary items. The corresponding reported activity uncertainties do not include geometry parameter uncertainties, such as activity distribution, dimensions, and densities. These uncertainties can be of the order of 50% (Dyrcz et al., 2021). The GS results relative differences, before and after melting, are around 25% for ^{60}Co, while they are much larger for other radionuclides. Hence, the ^{60}Co activity values are consistent for all waste packages and unitary items. Contrary to ^{60}Co, the other radionuclides have not been systematically identified in all waste packages and unitary items. Thus, the corresponding activities averaged over the total mass could deviate from the values after melting.

4. Conclusions

The activity values of the ETM radionuclides are evaluated via a qualified NDA technique, based on GS. The technique presents several challenges related to the accurate determination of the geometry modelling parameters, such as the activity distribution. Hence, the impact of the homogeneous activity distribution assumption within the primary waste (waste package) is investigated using the concept of geometry optimization methodology. The geometry optimization results allow establishing the optimized geometry models. It is achieved by constructing the FOMs that rely on the multi-count and multi-line activity consistencies. After the geometry optimization, the activity values of the opposite faces are consistent using the optimized models. Application of this NDA technique for waste packages and unitary items has shown that multi-count activity ratios of the reference and optimized geometry models range from 0.92 to 1.34. It demonstrates that the uncertainty associated with homogeneous activity distribution in the primary waste leads to consistent results for this type of waste. The activity values can be quantified by computing the average activity for all faces and considering the reference model. The obtained results allow confirming that the activity average over the faces, assuming

Table 8
Average activity values over two, four faces for reference and optimized models with uncertainties given at 1 σ for WP5.

WP5 CR-139255									
Radionuclide (Bq/g)	REFERENCE			OPTIMIZED			OPTIMIZED/REFERENCE		
	Faces 1–3	Faces 2–4	Four faces	Faces 1–3	Faces 2–4	Four faces	Faces 1–3	Faces 2–4	Four faces
^{60}Co	2.14E+02 (1%)	2.27E+02 (1%)	2.21E+02 (1%)	2.68E+02 (1%)	2.71E+02 (1%)	2.69E+02 (1%)	1.25 (±0.02)	1.19 (±0.02)	1.22 (±0.02)
^{22}Na	4.28E−01 (4%)	5.75E−01 (4%)	5.01E−01 (3%)	4.87E−01 (4%)	7.94E−01 (4%)	6.41E−01 (3%)	1.14 (±0.07)	1.38 (±0.08)	1.28 (±0.05)
^{42}K	5.24E−01 (7%)	5.35E−01 (7%)	5.29E−01 (5%)	8.64E−01 (7%)	5.78E−01 (7%)	5.71E−01 (5%)	1.08 (±0.10)	1.08 (±0.11)	1.08 (±0.07)
^{44}Sc	2.47E+00 (2%)	3.51E+00 (2%)	2.99E+00 (2%)	2.60E+00 (2%)	4.64E+00 (2%)	3.62E+00 (2%)	1.05 (±0.04)	1.32 (±0.04)	1.21 (±0.03)
^{54}Mn	1.95E+00 (3%)	2.49E+00 (3%)	2.22E+01 (2%)	2.44E+00 (3%)	2.75E+00 (2%)	2.59E+00 (2%)	1.25 (±0.06)	1.10 (±0.05)	1.17 (±0.04)
^{57}Co	NA								

Table 9
List of identified radionuclides with the activity values for the two or four faces of the unitary items. The uncertainties are quoted at 1 σ (relative uncertainties). MDA values are in *italic*. NA indicates that no measurement was performed for the face.

	CR-063808	CR-W13057	CR-065037		CR-065038	
	^{60}Co (Bq/g)	^{60}Co (Bq/g)	^{60}Co (Bq/g)	^{44}Sc (Bq/g)	^{60}Co (Bq/g)	^{44}Sc (Bq/g)
FACE 1	1.89E+01 (20.5%)	5.88E+00 (21%)	3.78E+00 (2%)	*5.910E−02*	1.15E+01 (1.9%)	8.71E−02 (13.3%)
FACE 2	1.01E+01 (20.5%)	2.24E+01 (20.5%)	NA	NA	NA	NA
FACE 3	2.02E+01 (20.5%)	5.37E+00 (20.5%)	4.37E+00 (2%)	2.86E−02 (24%)	1.4E+01 (1.9%)	1.26E−01 (11.5%)
FACE 4	7.08E+01 (20.5%)	3.69E+00 (21%)	NA	NA	NA	NA
Activity ratio between faces 1 and 3	1.07 (± 0.31)	1.09 (± 0.32)	1.15 (± 0.03)		1.21 (± 0.03)	1.45 (± 0.26)
Activity ratio between faces 2 and 4	6.99 (± 2.02)	6.08 (± 1.76)				
Average activity over all faces	3.0E+01 (13%)	9.35E+00 (13%)	4.08E+00 (1%)		1.28E+01 (1%)	1.07E−01 (9%)
Estimated activity via AVG-DR	2.29E+02	5.06E+01	4.35E+01		8.72E+01	
Net mass kg , density g/cm^3	909.5, 0.65	905, 0.66	1324, 1.18		1315, 1.17	

Table 10
Average activity values over two, four faces for reference and optimized models with uncertainties given at 1 σ for UP1.

UP1 CR-063808									
Radionuclide (Bq/g)	REFERENCE			OPTIMIZED			OPTIMIZED/REFERENCE		
	Faces 1–3	Faces 2–4	Four faces	Faces 1–3	Faces 2–4	Four faces	Faces 1–3	Faces 2–4	Four faces
^{60}Co	1.96E+01 (14%)	4.05E+01 (18%)	3.00E+01 (13%)	2.16E+01 (15%)	3.38E+01 (15%)	2.77E+01 (11%)	1.11 (±0.23)	0.83 (±0.19)	0.92 (±0.15)

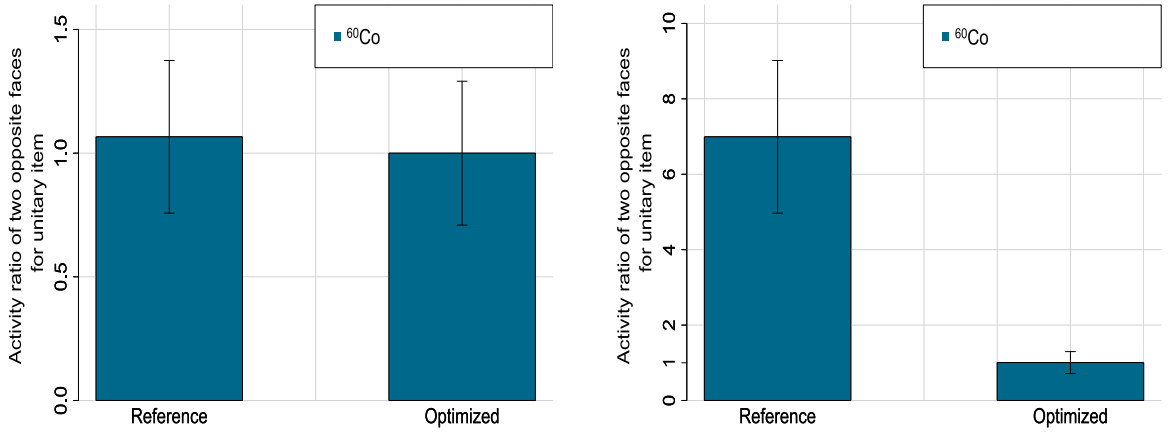

(a) Faces 1 and 3. (b) Faces 2 and 4.

Fig. 4. Activity ratios for opposite faces before and after optimization for UP1 CR-063808.

uniform activity distribution, is suitable compared with the geometry optimization results.

The waste packages and unitary items analysed above are subjected to elimination via melting. The melting process does not allow correlating the samples after melting to waste packages and unitary items individually. Hence, we compare the AVG activities of all samples to the averaged values over all primary waste (waste package and unitary items). The results show that the AVG activity values before melting are consistent with the corresponding values after melting, especially for the dominant ^{60}Co, which is identified in all primary waste.

Table 11
Average activity values over two, four faces for reference and optimized models with uncertainties given at 1 σ for UP2.

	UP2 CR-W13057								
Radionuclide (Bq/g)	REFERENCE			OPTIMIZED			OPTIMIZED/REFERENCE		
	Faces 1–3	Faces 2–4	Four faces	Faces 1–3	Faces 2–4	Four faces	Faces 1–3	Faces 2–4	Four faces
^{60}Co	5.63E+00 (14%)	1.31E+01 (18%)	9.35E+00 (13%)	6.25E+00 (15%)	1.52E+01 (15%)	1.07E+01 (11%)	1.11 (±0.23)	1.16 (±0.27)	1.15 (±0.20)

Table 12
Average activity values over two faces for reference and optimized models with uncertainties given at 1 σ for UP3 and UP4.

Radionuclide (Bq/g)	UP3 CR-065037			UP4 CR-065038		
	REFERENCE	OPTIMIZED	OPTI-MIZED/REFERENCE	REFERENCE	OPTIMIZED	OPTI-MIZED/REFERENCE
	Faces 1–3	Faces 1–3	Faces 1–3	Faces 1–3	Faces 1–3	Faces 1–3
^{60}Co	4.08E+00 (1%)	4.49E+00 (1%)	1.10 (±0.02)	1.28E+01 (1%)	1.38E+01 (1%)	1.08 (±0.02)
^{44}Sc				1.07E−01 (9%)	1.09E−01 (7%)	1.03 (±0.11)

Table 13
List of identified radionuclides with the activity values for the six samples. The uncertainties are quoted at 1 σ (relative uncertainties).

Sample ID	Mass (g)	^{60}Co (Bq/g)	^{44}Sc (Bq/g)	^{44}Ti (Bq/g)	^{54}Mn (Bq/g)
PSAM-000958	84	1.32E+02 (2%)	1.94E+00 (5%)	2.07E+00 (8%)	7.06E−01 (12%)
PSAM-000959	84	1.30E+02 (2%)	1.87E+00 (6%)	1.63E+00 (9%)	7.12E−01 (11%)
PSAM-000960	82	1.51E+02 (2%)	6.48E−01 (12%)	5.65E−01 (15%)	1.27E+00 (8%)
PSAM-000961	80	1.56E+02 (2%)	5.68E−01 (16%)	4.12E−01 (20%)	1.48E+00 (7%)
PSAM-000962	82	1.22E+02 (2%)	7.73E−01 (12%)	1.16E+00 (12%)	2.06E+00 (6%)
PSAM-000963	82	1.22E+02 (2%)	7.84E−01 (11%)	9.5E−01 (12%)	1.95E+00 (6%)

Table 14
Average activity values in Bq/g with uncertainties given at 1 σ of the waste before and after melting.

Radionuclide (Bq/g)	Before melting	After melting	Before/After
^{60}Co	1.69E+02 (1%)	1.35E+02 (1%)	1.25 (± 0.01)
^{44}Sc	2.06E+00 (6%)	1.11E+00 (3%)	1.87 (± 0.13)
^{44}Ti	4.40E+00 (2%)	1.14E+00 (4%)	3.86 (± 0.18)
^{54}Mn	3.28E+00 (2%)	1.36E+00 (3%)	2.42 (± 0.09)

Additionally, this paper presents the methodology that allows performing a preliminary quantification of the specific activities of ^{60}Co for operational waste package production purposes. It is based on the experimental correlation between the ratio of the specific activity of ^{60}Co and the AVG-DR as a function of the apparent density of the waste item. This methodology is valid under the assumption that ^{60}Co is the dominant gamma dose contributor in the waste item, where the decay time is more than 3 years. This methodology allows optimizing dose exposure and utilizing resources to guarantee the conformity of the waste packages to the criteria of the melting facility.

Finally, this paper presents the results of a pilot campaign for the treatment and elimination process of CERN's metallic LILW waste by melting. A pilot batch of 19 m^3 of metallic LILW waste was successfully melted at the end of 2022, resulting in 3 melting baths (around 4 tons each). The melted waste was disposed of in the French final repository by June 15 2023, marking the pilot project's end. The melting project has been a key contributor to the opening of an efficient elimination pathway for the yearly disposal of up to 16 m^3 of LILW metallic waste in France. Future plans include applying the developed methodology to future waste.

CRediT authorship contribution statement

Patrycja Dyrcz: Writing – review & editing, Writing – original draft, Visualization, Validation, Methodology, Investigation, Formal analysis, Data curation, Conceptualization. **Nabil Menaa:** Writing – review & editing, Supervision, Methodology, Conceptualization. **Matteo Magistris:** Writing – review & editing, Supervision. **Chris Theis:** Writing – review & editing, Resources. **Luca Bruno:** Resources, Project administration. **Gerald Dumont:** Resources, Project administration. **Renaud Charousset:** Resources.

Declaration of competing interest

The authors declare that they have no known competing financial interests or personal relationships that could have appeared to influence the work reported in this paper.

Data availability

The authors do not have permission to share data.

References

Accord, 2011. Accord entre le Conseil Fédéral Suisse, le Gouvernement de la République Française, et l'Organisation Européenne pour la Recherche Nucléaire relatif à la Protection contre les rayonnements ionisants et à la Sûreté des Installations de l'Organisation Européenne pour la Recherche Nucléaire, conclu le 15 novembre 2010, entré en vigueur par échange de notes le 16 septembre 2011. RS 0.814.592.2, Recueil Officiel n. 34 du 23 août 2011, page 3825. Décret n. 2011-1024 du 24 août 2011, JORF n. 0199 du 28 août 2011 page 14594.

ANDRA, 2013a. Critères radiologiques d'acceptation des déchets TFA. SUR.SP.AMES.02.0007.

ANDRA, 2013b. Specification d'acceptance des colis de dechets radioactifs au CSFMA. INB N 149.ACO.SP.ASRE.99.0002.D.

Assad, Ali, Chiron, Maurice, Nimal, Jean Claude, Diop, Cheikh M'backé, Ridoux, Philippe, 2000. General formalism for calculating Gamma-ray buildup factors in multilayer shields into MERCURE-6 code. J. Nucl. Sci. Technol. 37 (sup1), 493–497. http://dx.doi.org/10.1080/00223131.2000.10874935, arXiv:10.1080/00223131.2000.10874935.

Bronson, F., 1997. ISOCS, A laboratory quality ge Gamma spectroscopy system you can take to the source for immediate high quality results. In: Proceedings of the Rapid Radioactivity Measurements in Emergency and Routine Situations Conference, UK, October.

Bronson, F., 2008. Uncertainty of gamma-ray spectrometry measurement of environmental samples due to uncertainties in matrix composition, density and sample geometry. Appl. Radiat. Isot. (ISSN: 0969-8043) 276, 589–594. http://dx.doi.org/10.1007/s10967-008-0604-z, URL https://link.springer.com/article/10.1007%2Fs10967-008-0604-z#article-info.

Dyrcz, Patrycja, 2022. Radiological characterization of low- and intermediate level (LL/IL) radioactive waste. URL https://cds.cern.ch/record/2837007, Presented 06 Sep 2022.

Dyrcz, Patrycja, Frosio, Thomas, Menaa, Nabil, Magistris, Matteo, Theis, Chris, 2021. Qualification of the activities measured by gamma spectrometry on unitary items of intermediate-level radioactive waste from particle accelerators. Appl. Radiat. Isot. 167, 109431. http://dx.doi.org/10.1016/j.apradiso.2020.109431.

Forkel-Wirth, Doris, Roesler, Stefan, Silari, Marco, Streit-Bianchi, Marilena, Theis, Christian, Vincke, Heinz, Vincke, Helmut, 2013. Radiation protection at CERN. http://dx.doi.org/10.5170/CERN-2013-001.415, arXiv:1303.6519, URL https://cds.cern.ch/record/1533023, Comments: 22 pages, contribution to the CAS - CERN Accelerator School: Course on High Power Hadron Machines; 24 May - 2 Jun 2011, Bilbao, Spain.

Frosio, Thomas, Menaa, Nabil, Bertreix, Philippe, Rimlinger, Maeva, Theis, Chris, 2020. A novel technique for the optimization and reduction of gamma spectroscopy geometry uncertainties. Appl. Radiat. Isot. (ISSN: 0969-8043) 156, 108953. http://dx.doi.org/10.1016/j.apradiso.2019.108953, URL https://www.sciencedirect.com/science/article/pii/S0969804319306852.

Kaminski, S., Jakobi, A., Wilhelm, Chr., 2014. Uncertainty of gamma-ray spectrometry measurement of environmental samples due to uncertainties in matrix composition, density and sample geometry. Appl. Radiat. Isot. (ISSN: 0969-8043) 94, 306–313. http://dx.doi.org/10.1016/j.apradiso.2014.08.008, URL https://www.sciencedirect.com/science/article/pii/S0969804314003091.

Menaa, N., Bosko, A., Bronson, F., Venkataraman, R., Russ, W.R., Mueller, W., Nizhnik, V., Mirolo, L., 2011. Mathematical efficiency calibration with uncertain source geometries using smart optimization. In: 2011 2nd International Conference on Advancements in Nuclear Instrumentation, Measurement Methods and their Applications. pp. 1–7. http://dx.doi.org/10.1109/ANIMMA.2011.6172913.

TECDOC IAEA, 2007. Strategy and Methodology for Radioactive Waste Characterization. Number 1537, Vienna, ISBN: 92-0-100207-6, URL https://www.iaea.org/publications/7655/strategy-and-methodology-for-radioactive-waste-characterization.